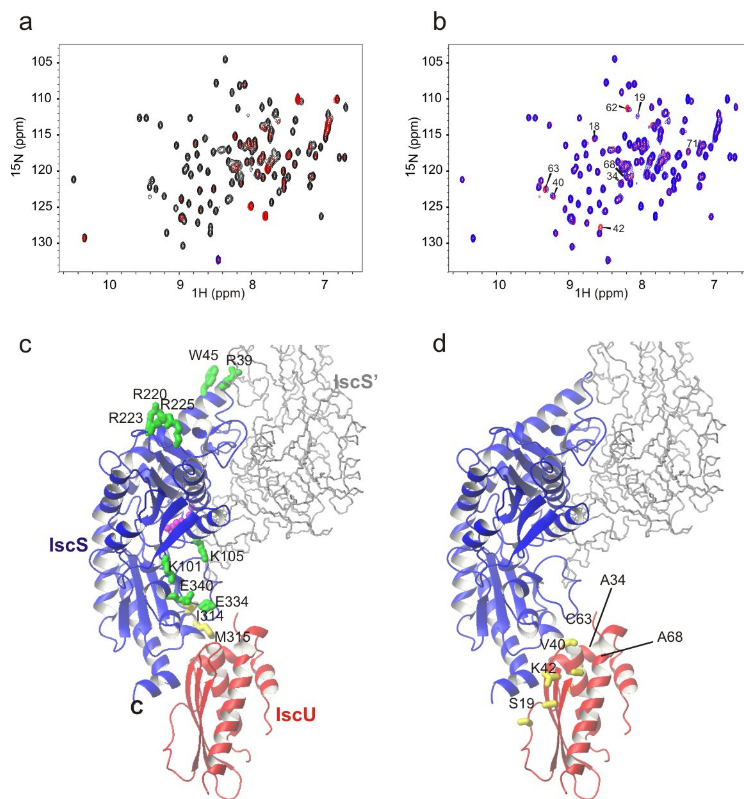

Supplementary Figure S1 – Validating our approach with the IscS/IscU binary complex. a) Comparison of the NMR HSQC spectra of ^{15}N-labelled IscU in the absence (black) and in the presence (red) of wild-type IscS (1:1 molar ratio). b) As in a) but IscU was recorded in the absence (blue) and in presence (red) of unlabeled IscS_I314E_M315E (1:1 molar ratio). c) Mapping of the IscS mutants onto the 3LVL structure. IscS ribbon is in blue, IscU in red. PLP is shown in magenta. Mutation of I314 and M315 (yellow side chains) into glutamates weakens IscS binding. All the other mutations (green side chains) have no effects. d) Mapping of the IscU resonances affected in b) onto the structure of IscU using the 3LVL coordinates and the same orientation and color coding as in c). The side chains of the affected residues are in yellow.

Protein	C, mg/ml	R_g, Å	D_{max}, Å	V_p, 10^{-3} Å^3	MM_{SAXS}, kDa	MM_{exp} kDa	χ_{ab}	χ_{rb}
IscS	2.5÷5.0	31.0±0.4	109±5	144±20	85±10	90.180	1.09	1.25
IscU	5.0	18.1±0.3	64±5	27±5	13±4	13.849	1.03	1.48
CyaY	5.0	15.2±0.3	50±3	25±5	12±4	12.231	1.01	1.20
IscS/IscU	2.5÷5.0	35.0±0.5	121±5	162±20	112±10	117.878	1.21	1.50
IscS/CyaY	2.5÷5.0	31.1±0.4	109±5	155±20	105±10	114.642	1.08	1.85
IscS/IscU/CyaY	2.5÷5.0	34.1±0.5	119±5	182±20	122±10	142.34	1.18	1.78

Notes: C, protein concentrations; R_g, radius of gyration; D_{max}, maximum size of the particle, V_p, excluded volume of the hydrated particle, MM_{exp} experimental molecular mass of the solute and χ_{ab} and χ_{rb} values for the fit curves from *ab initio* models and from high resolution models (for proteins alone) and rigid body modeling (for complexes) using CRYSOL/SASREF, respectively.

Supplementary Table S1 - Summary of the SAXS data.

IscS Mutant	IscU	CyaY	TusA	Method
R39E	++	+	n.d.	Pull-down
W45R	++	++	-	Pull-down
E49A	++	n.d.	-	Pull-down
D52A/R/Y/M	++	++/n.d.	-	Pull-down
D65F	++	++	+	Pull-down
F89E	++	n.d.	n.d.	Pull-down
R112E	++	n.d.	n.d.	Pull-down
R116E	++	+	++	Pull-down
R220E	++	-	++	Pull-down
R223E	n.d.	-	n.d.	Pull-down
G234L	++	+	n.d.	Pull-down
E311R	++	n.d.	n.d.	Pull-down
A327V	+	+	++	Pull-down
C328S	++	n.d.	n.d.	Pull-down
R340E	++	-	+	Pull-down
D346R	++	n.d.	n.d.	Pull-down
L386R,	++	n.d.	n.d.	Pull-down
M389R	++	n.d.	n.d.	Pull-down
R223E/R225E	++	n.d.	n.d.	Pull-down
R225E/E227R	++	-	++	Pull-down
R237E/M239E	++	-	n.d.	Pull-down
R39E/W45E	++	++	n.d.	NMR
K101E/K105E	++	++	n.d.	NMR
R220E/R223E/R225E	++	-	n.d.	NMR
I314E/M315E	+	++	n.d.	NMR
E334S/R340S	++	++	n.d.	NMR

Note: The only noticeable difference between the pull-down data and ours is the R340E mutant which abolishes CyaY binding whereas the milder double mutant IscS_E334S/R340S retains binding. By introducing a negatively charged group, the R340E mutant could have a destabilizing effect for the protein fold.

Supplementary Table S2 - Experimental validation of the SAXS models. The symbols ++, + and - correspond to mutations which retain, weaken or abolish binding as judged from pull-down[56] or NMR (our own data) experiments as specified in the last column. N.d. stands for not determined.

Supplementary Discussion

Validation of our approach using the IscS/IscU complex

We applied the same approach used for the CyaY binary and ternary complexes to IscS/IscU. The model built from SAXS data collected on the IscS/IscU complex was refined using restraints obtained from mutagenesis and NMR titrations. We mapped the interaction of IscU on the IscS surface using the IscS mutants produced for probing interaction with CyaY. First, we titrated ^{15}N labeled IscU with wild-type IscS for reference. The spectrum of IscU disappears completely at a 1:1 molar ratio, as expected for a relatively stable 110 KDa complex, but without any previous resonance broadening or chemical shift perturbation (Supplementary Figure S1a). This behavior is typical of complexes in the low exchange regime[57]. Unfortunately, while indicating the quantitative formation of a complex, this behavior did not allow us to obtain information on the IscU residues affected by binding.

The IscS mutants produced effects indistinguishable from the wild-type indicating that the mutations do not interfere with binding, with the only exception for IscS_I314E/M315E. Titration of this mutant into labeled IscU caused small but clear chemical shift perturbation of the ^{15}N-labeled IscU spectrum (Supplementary Figure S1b). The different behavior is likely to be due to a different exchange regime that must reflect a reduced affinity of this complex.

These results determined the position of IscU close to the IscS C-terminus (Supplementary Figure S1c). The possibility of observing chemical shift perturbation with the IscS_I314E/M315E mutant also allowed us to identify the residues of IscU involved in binding. Mapping the chemical shift perturbation onto the IscU structure shows that the residues affected are Gly18, Ser19, Ala34, Val40, Lys42, Gly62, Cys63, Ala68, and Ser71 (Supplementary Figure S1d).

The surfaces of interactions both on IscS and IscU identified with this approach are in full agreement with the high resolution crystal structure of IscS/IscU[56] which appeared only after we had concluded this part of the project, thus giving us an independent confirmation of the sensitivity of the method and the reliability of our conclusions.

Supplementary References

56. Shi, R. et al. Structural basis for Fe-S cluster assembly and tRNA thiolation mediated by IscS protein-protein interactions. *PLoS Biol* **8**, e1000354 (2010).
57. Neuhaus, D. & Williamson, M. P. The Nuclear Overhauser Effect In Structural And Conformational Analysis (Wiley-vch Verlag Gmbh, 2000).